A major hydrobiological change in Dasht-e Arjan Wetland (SW Iran) during the late glacial-early Holocene transition revealed by subfossil chironomids

Cyril Aubert[1*]**, Morteza Djamali**[1,2]**, Matthew Jones**[3]**, Hamid Lahijani**[2]**, Nick Marriner**[4]**, Abdolmajid Naderi-Beni** [2]**, Arash Sharifi**[5]**, Philippe Ponel**[1]**, Emmanuel Gandouin**[1]

1 CNRS, IRD, Aix Marseille Univ, Avignon Université, IMBE, Aix en Provence, France

2 INIOAS (Iranian National Institute for Oceanography and Atmospheric Sciences), No.3, Etemad Zadeh St., Fatemi Ave., Tehran, Iran, 1411813389, 14155-4781

3 School of Geography, University of Nottingham, University Park, Nottingham. NG7 2RD UK

4 Laboratoire de Chrono-Environnement, CNRS, Besançon, France

5 Halophytes and C4 Plants Research Laboratory, Department of Plant Science, School of Biology, University of Tehran, Tehran, Iran

*Corresponding author: cyril.aubert@imbe.fr

16   **Abstract**

17   The late glacial-early Holocene transition is a key period in the Earth's history. However, although this transition is

18   well studied in Europe, it is not well constrained in the Middle East and palaeohydrological records with robust chronologies

19   remain scarce from this region. Here we present an interesting hydrobiological record showing a major environmental change

20   occurring in the Dasht-e Arjan Wetland (SW Iran, near to Persepolis) during the late glacial-early Holocene transition (*ca.*

21   11,650 years cal BP). We use subfossil chironomids (Insecta: Diptera) as a proxy for hydrological changes and to reconstruct

22   lake-level fluctuations. The Arjan wetland was a deep lake during the Younger Dryas (YD) marked by a dominance of

23   *Chironomus plumosus/anthracinus*-type, taxa adapted to anoxic conditions of deep waters. At the beginning of the Holocene a

24   drastic decrease (more than 80% to less than 10%) of *Chironomus plumosus/anthracinus*-type, combined with diversification

25   of littoral taxa such as *Polypedilum nubeculosum*-type, *Dicrotendipes nervosus*-type and *Glyptotendipes pallens*-type suggest

26   a lake-level decrease and a more vegetalized aquatic environment. We compare and contrast the chironomid record of Arjan

27   with a similar record from northwestern Iran. The palaeoclimatic significance of the record, at a local and regional scale, is

28   subsequently discussed. The increase in northern hemisphere temperatures, inferred by geochemical data from NGRIP, at the

29   beginning of the Holocene best explains the change from the YD highstand to early Holocene lowstand conditions in the Dasht-

30   e Arjan wetland. However, a contribution of the melt-water inflow from small local glaciers in the catchment basin is not

31   excluded.

32

33   **Key words:** Younger Dryas, Climate change, Karst, Lake-level change, Zagros, late glacial-early Holocene transition, Iran,
34   Middle East.

35

36

Introduction

The late Pleistocene to early Holocene transition marks the final part of the "Last Glacial-Interglacial Transition" (LGIT) or "Last Termination" (Lowe and Walker 1997; Hoek 2008). It is a key event in the Earth's history characterized by a series of climatic changes of high magnitude that provide the possibility to investigate the mechanisms responsible for abrupt climatic changes (Hoek 2008). In the North Atlantic region, a detailed spatio-temporal framework is now available for the patterns of hydroclimatic and biotic changes during this transition (e.g. Ammann et al. 2000; Rasmussen et al. 2006). The biotic responses to late glacial-early Holocene climatic changes display many spatial discrepancies highlighting the important role of local ecological conditions such as lake topography and the composition of aquatic macrophyte communities (Engels and Cwynar, 2011). In the low temperate to subtropical latitudes of SW Asia, the late glacial hydroclimatic changes are still poorly understood compared to Europe and the Mediterranean. In the Middle East, for instance, the more complex interactions between climatic systems can potentially cause more multifaceted responses of biomes to hydroclimatic variations (Djamali et al. 2010). Furthermore, this is a key period during which nomadic hunter-gatherers sedenterized to form the first farming communities (Blockley and Pinhasi 2011; Willcox 2012). In this regard, the Zagros-Taurus Mountains in western Iran and southeastern Turkey is a key region in understanding the Neolithisation process (Matthews and Fazeli 2013). A recent discovery of the cultivation of wild cereals in the foothills of the Zagros Mountains in Iran (Riehl et al. 2013), at the very onset of the Holocene, suggests that this area should also be considered as one of the earliest centers for cereal and pulse domestication in the Middle East. In addition, the study of ancient DNA of human remains dating to Early Holocene suggests that the Zagros Mountains constitute the major center of eastward expansion of early farming communities (Broushaki et al. 2016). Unraveling the hydroclimatic changes associated with these events is thus important in understanding and in contextualizing the possible environmental changes responsible for the early Neolithisation of the region.

63   In the Middle East, although palaeohydrological records are available from NW Zagros, E

64   Anatolia, Caucasus and the Talesh Mountains (e.g. Stevens et al. 2006; Sharifi et al. 2015; Aubert et al.

65   2017), no high-resolution record is available from the central-southern Zagros for the late glacial-early

66   Holocene transition. The present study provides a hydrological record for this transition in the southern

67   Zagros based on lacustrine deposits of the Dasht-e Arjan Wetland. Chironomid head capsules, which

68   have been demonstrated to be good palaeo-temperature and palaeosalinity indicators (Heiri et al. 2011;

69   Eggermont et al. 2006; Zhang et al. 2007), are also powerful proxies to reconstruct lake-level

70   fluctuations (Eggermont et al. 2007). Recently, they have further been suggested as a promising proxy

71   to reconstruct changes in precipitation seasonality in the semi-arid region of the Middle-East (Aubert et

72   al. 2017). We place the new Arjan record in a regional context. We compare and contrast it with

73   hydroclimatic changes of central Asia and Eastern Mediterranean, to further our regional understanding

74   of ecosystem responses to this key climatic transition.

75

76   Materials and methods

77

78   *Study area*

79   Very little information is available from the wetland of Dasht-e Arjan (Plain of Arjan). The wetland (N

80   29°36'38", E 51°59'04", 1,984 m asl; Fig. 1) is located *ca*. 50 km to the west of Shiraz. It is a relatively

81   large, moderately saline lake located near Lake Parishan with which it forms a Wetland of International

82   Importance (Ramsar Site no. 37; https://www.ramsar.org). The climate of Shiraz (1,540 m asl) is of

83   continental Mediterranean-type (Djamali et al. 2011) with most of the precipitation falling during the

84   winter months (Fig 1C). Apart from the direct precipitation in its catchment basin, a major source for

85   Dasht-e Arjan Wetland is the Arjan spring, which has a discharge rate fluctuating between 750 l/s and

86   100 l/s (Milanovic and Aghili 1990).

87   Although located within the Zagros Fold Belt, the Dasht-e Arjan region is situated in a local extensional

88   tectonic setting which has created a subsiding sedimentary basin. The subsidence is controlled by the

89   activity of two normal faults called the West Arjan Fault (N45°, 78°SE) and the East Arjan Fault (N55°,

90 70NW) which have created the 100-500 m high and ~10 km long SW-NE trended almost vertical cliffs

91 composed mainly of Oligocene-Miocene Asmari Limestone formation to the west and east of the

92 wetland (Fig. 1B; Seyrafian et al. 2011). Hydrogeologically, the Dasht-e Arjan Wetland seems to be

93 located in a "polje" (a flat karstic plain) whose waters are evacuated through a "ponor" (an opening in

94 the bottom of a polje), of 10-15 meter diameter, into a karstic subterraneous system during highstands

95 with possible hydrological connection to the Kazerun (Lake Parishan) basin (Milanovic and Aghili

96 1990).

97 **Fig. 1**

98

99 *Coring, lithostratigraphy and radiocarbon dating*

100 Coring was performed using a Cobra vibracorer, allowing to gather 10 successive core sections of 1-m

101 length and 5-cm width from the southeastern corner of the lake (29°35'33"N, 51°59'03"E, 1,992m asl)

102 near the location of the "ponor" (Fig. 1B). The maximum depth attained was 960 cm. The

103 lithostratigraphy comprises three major units: (1) a basal unit dominated by calcareous clayey mud with

104 traces of pedogenesis; (2) middle section dominated by bioclastic calcareous mud; and (3) the upper unit

105 dominated by organic-rich calcareous mud (Fig. 2; upper right). Six samples composed of bulk (peat

106 and gyttja) and plant remains (fibers) were AMS radiocarbon dated at Poznan Radiocarbon Laboratory

107 (Table 1). The radiocarbon ages were calibrated using Intcal13 calibration curve (Reimer et al. 2013) in

108 the Clam package (Blaauw 2010) run in R software version 3.2.2 (R Core Team 2012). The age-depth

109 model is based on linear interpolation taking into account the probability distribution of the calibrated

110 ages (Fig. 2). Two radiocarbon ages were excluded from the age-depth model (sample Poz-Arj478 at

111 478 cm and sample Poz-Arj756 at 756 cm depth; Table 1). These two samples are outliers. The first

112 sample is too old, possibly because of the old carbon found in the bulk sediment composed of calcareous

113 mud, a sediment composition which tends to yield "older" ages (Table 1). The second sample is too

114 young, most probably because it is composed of root and rootlets penetrating into old sediment from the

115 much younger plants. The palustrine sedimentary facies which incorporates this sample display

116   abundant root traces, corroborating this assumption (Fig. 2). A recent publication by Djamali et al.

117   (2018) has shown that similar age inversions (too young ages) have also been reported from a palustrine

118   carbonate facies in the western Persepolis basin. We have retained the ages provided by the samples

119   Poz-Arj503, Poz-Arj614 and Poz-Arj671 because they are composed of *in situ* organic matter (gyttja to

120   very fine grained peat), formed within the aquatic environments through biological processes. All

121   carbonate content was removed through a chemical treatment at the radiocarbon laboratory of Poznan

122   (T. Goslar, personal communication) diminishing the possible contamination by old carbon originating

123   from geological formations. We consider that the age Poz-Arj614 giving a 2-σ range age of 11 631-12

124   060 is a very reliable age and marks the second part of the Younger Dryas, just before the onset of the

125   Holocene. This age range is also displayed in the chironomid diagram of Fig. 3 (see discussion).

126   *Chironomid analysis*

127   Sixteen sediment samples weighing between 40 to 90 g were analyzed for chironomids, every

128   5 cm, along the fossiliferous interval of 630 to 550 cm. The laboratory methods used for extraction and

129   identification of the chironomid subfossil head capsules are described in Gandouin et al. (2005). To

130   summarize, the extraction consisted of KOH-deflocculation, water-washing over a 100 µm sieve and oil

131   flotation. A minimum of 50 head capsules per sample is required to provide statistically significant

132   estimates of ecological conditions (Heiri and Lotter 2001). Identification criteria of head capsules are

133   based on a Palearctic dichotomous key developed by Brooks et al. (2007). The chironomid abundance

134   diagram was created using C2 software version 1.7.2 (Juggins 2007).

135

136   *Multivariate analyses of sub-fossil chironomid data*

137   A constrained sum-of-squares cluster analysis (CONISS) for percentage data was performed with R

138   (version 3.2.2) and the package "rioja" (Juggins 2017) to highlight major changes in chironomid

139   assemblage composition throughout the stratigraphy (Grimm 1987). Principal Component Analysis

140   (PCA) (Fig. 3) was performed on a data percentage matrix of 9 taxa for 16 samples. The PCA was

141   carried out with "ade4" and "vegan" packages in R software (R Core Team 2012). Beforehand, data

142 were square-root transformed with the aim of stabilizing the variance. Rare taxa (present in only one

143 sample or with a relative abundance always <5 %) were excluded from analyses.

144

145 Results and interpretation

146 For the chironomid analysis, only the section between 630 and 550 cm was used because it corresponds

147 to the late glacial-early Holocene transition and presents almost the only interval with sufficient

148 chironomid head capsules for statistical analyses. Interestingly, this sequence of 0.80 meter corresponds

149 to the end of the Younger Dryas and the onset of the Holocene (6.30-5.50 m: 12,380 to 10,103 years cal

150 BP; Fig. 2). Fig. 3 presents a simplified diagram of chironomid relative abundances (in %). CONISS

151 analysis revealed three faunal assemblage zones that we designate as Ach1: 630-605 cm (12,380-11,650

152 years cal BP), Ach2: 605-563 cm (~11,650-10,470 years cal BP) and Ach3: 563-555 cm (10,470-10,100

153 years cal BP). To the right of the chironomid diagram, percentage variations of a selection of pollen taxa

154 have also been presented, based on a recently published pollen diagram from the same study core

155 (Hosseini et al. 2017).

156 **Fig. 2**

157

158 *Ach1: 630-605 cm (12,380-11,650 years cal BP):*

159 This zone is dominated by *Chironomus plumosus*/*anthracinus*-type and significant presence of

160 *Psectrocladius psilopterus*-type (Fig. 3). Together, these two chironomid taxa constitute up to 90% of

161 the chironomid assemblage (Fig. 3). PCA scores for these chironomid taxa and the samples containing

162 them are both positioned on the positive side of the PCA axis1 between 0.5 and 1 (Fig. 4).

163   The Ach1 upper boundary closely mirrors the ARJp1 pollen assemblage zone (Fig. 3, right

164 panel). This pollen zone is characterized by the dominance of pollen produced by very dry steppe plants

165 (Amaranthaceae, *Artemisia*) low values of *grasses* (Poaceae) and the total absence of trees. Only towards

166 its end do aquatic plants (Cyperaceae) and algae increase (*Botryococcus* and *Pediastrum*).

167

168   *Ach2: 605-563 cm (~11,650-10,470 years cal BP):*

169   A remarkable faunal change occurs in this zone with a drastic reduction in *Chironomus*

170   *plumosus/anthracinus*-type (Fig. 3) and, to a lesser extent, in *Psectrocladius psilopterus*-type

171   percentages (from 80-90% to below 10% for the latter taxa). By contrast, other taxa such as *Polypedilum*

172   *nubeculosum*-type, *Dicrotendipes nervosus*-type and *Glyptotendipes pallens*-type previously absent or

173   in low abundances in the record, become the dominant chironomid assemblages. *Procladius* spp.

174   percentages also increase during this zone. PCA axis1 scores follow the same trend as for *Chironomus*

175   *plumosus/anthracinus*-type and decrease markedly to around -1 during most of the upper part of the

176   zone (see Fig. 3).

177   Ach2 chironomid zone mostly correlates with ARJp2 pollen assemblage zone, characterized by

178   a sudden drop and then low values of Amaranthaceae and the dominance of grasses and semi-continuous

179   presence of aquatic plants (Cyperaceae and *Sparganium*-type) and algae (*Botryococcus* and

180   *Pediastrum*). Tree pollen appear in the diagram although with low values. A treeless grass-dominated

181   steppe with moderately developed aquatic vegetation is inferred (Hosseini et al., 2017).

182

183   *Ach3: 563-555 cm (10,470-10,100 years cal BP):*

184   During this zone, a slight rise of *Chironomus plumosus/anthracinus*-type and *Psectrocladius*

185   *psilopterus*-type and a decrease of *Polypedilum nubeculosum*-type is observed (Fig. 3). Other littoral

186   taxa such as *Dicrotendipes nervosus*-type and *Glyptotendipes pallens*-type are also present.

187   Furthermore, we note the emergence of *Xenochironomus* spp. from 565 cm. During Ach3 zone, PCA

188   axis1 scores increase slightly but remain negative (-0.5) at the top of sequence (Fig. 3).

189   Ach3 chironomid zone correlates with ARJp3 pollen assemblage zone in which grass pollen

190   abundances decrease while Pediastrum shows a peak. At the regional scale, a dry mountain steppe

191   vegetation and nutrient-rich mesotrophic conditions are inferred (based on *Pediastrum*).

192   **Fig. 3**

193

194   Statistically-based ecological groups of subfossil chironomids

195   PCA axis1 (56.2% of the total variance) opposes *Chironomus plumosus/anthracinus*-type on the positive

196   side (Fig. 4) to *Glyptotendipes pallens*-type, *Procladius* spp*., Polypedilum nubeculosum*-type,

197   *Tanytarsus* spp. and *Dicrotendipes nervosus*-type on the negative side. PCA axis 2 (17.3% of the total

198   variance) is characterized by a segregation between *Xenochironomus* spp. and *Psectrocladius*

199   *psilopterus*-type.

200   **Fig. 4**

201

202   Discussion

203   Chironomids as bathymetric bio-indicators

204   The PCA axis 1 clearly shows an opposition between *Chironomus plumosus/anthracinus*-type mostly

205   confined to the profundal zone of lakes (Brooks et al. 2007) against the inhabitants of littoral zone and

206   shallower water environments such as *Glyptotendipes pallens*-type and *Polypedilum nubeculosum*-type.

207   *Glyptotendipes pallens*-type is most often associated with aquatic macrophytes (Brooks et al. 2007;

208   Langdon et al. 2010). In fact, *Polypedilum nubeculosum*-type indicates relatively clear waters with

209   variable macrophyte density and/or high plant species richness (Langdon et al. 2010). *Chironomus*

210   *plumosus/anthracinus*-type are often associated with loose and fine-grained sediments such as mud and

211   silt (Henrikson et al. 1982; Brodin 1986). Among the *Chironomus* genera, many species are also adapted

212   to live and survive in deep waters, possibly hypoxic or anoxic conditions by producing a large amount

213   of hemoglobin (Brooks et al. 2007). It is well established elsewhere that chironomids are influenced by

214   lake bathymetry (Verneaux and Aleya 1998) and several transfer functions have been successfully

215   developed to reconstruct Holocene lake-level changes in Scandinavia (Luoto et al. 2018), in Canada

216   (Barley et al. 2006) and in China (Chang et al. 2017 and Wang et al. 2018).

217   Hence, PCA axis1 (Fig 4) may represent a bathymetric gradient with more positive scores

218   indicating higher lake levels, whereas more negative scores indicate a shallower lake and marshy

219   environments. Alternatively, the same trend may also indicate a transition from deep-water conditions

220   to marsh environments that is not necessarily related to lake-level fluctuations but to the development

221   of aquatic vegetation, from the littoral zone into the central lake basin. Either way, we consider the PCA

222   axis1 scores as an indicator for lake-level changes for the Arjan wetland (Fig 3). In this way, we find a

223   similar chironomid inferred hydrological dynamic already observed in Lake Neor (Fig. 5) located in

224   northwestern Iran (Aubert et al. 2017). At this latter site, high wetland moisture indicating more

225   permanent aquatic conditions are observed between 12,000 and 11,500 years cal BP. The wetland

226   moisture became low between 11,500 and 10,300 years cal BP (Aubert et al. 2017) with the increase in

227   semi-terrestrial taxa indicating ephemeral aquatic conditions on the lake margins.

228   The early Holocene section of our chironomid record shows a drastic fall in lake levels. This

229   suggests a major environmental change in less than 100 years (Fig. 3 and 5); indeed, the Arjan wetland

230   which was a deep lake during the Younger Dryas suddenly transformed into a shallow lake/marsh

231   environment with a well-developed aquatic vegetation at the onset of the Holocene, from *ca.* 11,600

232   years (see aquatic pollen increase in Fig. 3). Increase of *Procladius* spp. is compatible with lower lake

233   levels, since the members of this genus are carnivorous species (Brooks et al. 2007). In fact, in the

234   shrinking lake water bodies, the higher prey concentration may favor the predation regime. Later, a

235   decrease of *Polypedilum nubeculosum*-type and slight rise of *Chironomus plumosus/anthracinus*-type

236   at the very end of our chironomid record suggest a slight increase in lake levels between 10,350-10,100

237   years cal BP. The persistence of other lacustrine littoral taxa e.g. *Psectrocladius psilopterus*-type.,

238   *Dicrotendipes nervosus*-type and *Glyptotendipes pallens*-type confirms the presence of a well-

239   established aquatic vegetation, suggesting a relatively shallow lake/marsh environment. This notion is

240   supported by higher total organic content (TOC), higher carbon accumulation rates and lower $\delta^{13}C_{TOC}$

241   at Lake Neor, NW Iran (Sharifi et al. 2015). The appearance of *Xenochironomus* spp. (Fig. 3) is

242   imperatively associated with freshwater sponge (Pinder and Reiss 1983) also supporting the hypothesis

243   of lake level increase during this period. Higher annual temperatures could explain the higher organic

244   productivity in the Arjan wetland due to development of aquatic vegetation and its associated fauna (e.g.

245   *Dicrotendipes nervosus*-type, *Glyptotendipes pallens*-type) at the very beginning of the Holocene.

246

247   Palaeoclimatic implications

248   In summary, the dominance of *Chironomus plumosus*/*anthracinus*-type indicates the presence of a deep

249   and most probably stratified lake during Younger-Dryas in Dasht-e Arjan. Several hypotheses could

250   explain such a highstand in Arjan during the YD:

251   (i) The intensity of the Siberian High during the YD was higher compared to the early Holocene

252   (Mayewski et al. 1997; Sharifi et al. 2015). This would have pushed the westerlies to the south providing

253   precipitation over the central and southern Zagros (Sharifi et al. 2018). However, YD pollen

254   assemblages in Arjan are dominated by Amaranthaceae (Chenopodiaceae) with very low relative

255   abundances of Poaceae (Fig. 3), indicating the presence of a typical dry steppe developed under a dry

256   continental climate, exclude this first hypothesis.

257   (ii) Cooler summers during the YD in Northern Hemisphere could also explain higher moisture

258   levels in both Arjan and Neor wetlands. Low YD temperatures would have decreased annual lake water

259   evaporation. Evapo-transpiration was definitely lower under the generally colder temperatures of YD in

260   southern Iran. Fig. 5 compares the chironomid-based lake-level variations of Arjan Wetland (right) with

261   the NGRIP temperature record (North Greenland Ice Core Project members. 2004), and the Ti intensity

262   curve, dust flux concentration curve and the chironomid-based lake-level variations in Lake Neor in

263   northwestern Iran. It is interesting to note that the lake-level records in both Lake Neor and Arjan follow

264   the same trend, which inversely correlates with NGRIP temperature record, suggesting the significance

265   of low temperatures in maintaining high lake levels during the YD.

266

267   **Fig. 5**

268

269   (iii) Changes in the seasonality of precipitation, with increased rainfall during spring/summer

270   months, could also lead to more permanent lake conditions during summer months (Aubert et al. 2017).

271 Indeed, late spring precipitation will permit maintaining higher lake levels during summer and greater

272 humidity on lake margins. Nowadays, in the Arjan region, spring precipitation is lower than in

273 northwestern Iran (Djamali et al. 2012) and regional palaeoclimatic records do not suggest increased

274 spring/summer precipitation brought in by stronger monsoon conditions. They show that increased

275 summer precipitation only began around 11,000 years cal BP peaking at 10,000-6,500 years cal BP and

276 thus postdating the YD (Fleitmann et al. 2007). The hypothesis of a different precipitation seasonality

277 is not satisfactory in explaining the high lake levels at Arjan during the YD.

278 (iv) A further hypothesis, is the presence of small glaciers in the catchment area of Arjan due to

279 significant snowfall during the YD. Melt-waters would have maintained high lake levels during

280 summers. Although no study has so far reported the glacier extensions in the area, the available studies

281 on the last glacial maximum (LGM) glaciers in central Zagros suggest that the maximum descent of

282 glaciers has been at around 2,400 m elevation during the LGM (Ebrahimi & Seif 2016). Presence of

283 high mountains exceeding 2,600 m elevation in the lake catchment basin reinforces this hypothesis.

284 Indeed, glaciers at higher elevations could lead to year-round inflow, or at least summer round inflow

285 as they melt. This would be a distinct difference to Holocene conditions and would not necessitate a

286 change in rainfall seasonality, but would change inflow seasonality. It may also explain why the lake

287 levels fall after the transition to the Holocene, when all glaciers had already melted. A glacio-

288 geomorphological survey to attest the evidence of glacier extension in the Arjan area would be helpful

289 to investigate this. We therefore propose that a combination of lower evaporation due to lower annual

290 temperatures, still significant precipitation due to the occasional penetration of southward-pushed

291 westerlies into the southern Zagros (see Sharifi et al. 2018) and continuous glacier melting in the vicinity

292 of the wetland could explain the high lake levels of Arjan during the YD.

293 (v) Finally, the hydroclimatic processes may not have been the only factor controlling the lake-

294 level changes in Dasht-e Arjan. The complex karstic network of sinkholes in the southern part of the

295 wetland basin could also have played a role in water-level fluctuations. Today, during the highstands,

296 lake water is discharged through these karstic underground galleries preventing the lake level from

297 exceeding a certain altitude corresponding to the sinkhole system in the southeast corner of the basin.

298 The development of this karstic system and its connectivity to adjacent basins (e.g. Lake Parishan basin)

299 possibly accelerated at the beginning of the Holocene. If such a hypothesis is correct, it can be proposed

300 that the early Holocene lake levels would have been much higher if this karstic system had not

301 developed. High-resolution lake level fluctuations at Lake Parishan during the YD-early Holocene may

302 help to test this hypothesis e.g. by the detection of a synchronicity between the lake level fall in Arjan

303 and a lake level rise in Parishan.

304

305 Whatever the case, the YD lake highstand in Arjan adds to the complex hydrological history of

306 the Middle East at the late glacial-early Holocene transition. The hydrological history of each lake basin

307 should be studied by taking into consideration a number of different factors of which climatic change

308 constitutes just one component. For instance, comparing the hydrological evolution of two lake systems

309 in central Anatolia, both located in the same climatic context and most probably experiencing the same

310 hydroclimatic history, shows contrasting trends suggesting that climate was not the only factor

311 controlling lake-level changes. Site-specific factors should also be taken into account when interpreting

312 multi-proxy lake-level reconstructions (Roberts et al. 2016).

313 Dasht-e Arjan Wetland is located in a different climatic context compared to Anatolia and

314 Europe from which numerous lake level reconstructions are available. Moreover, it would have possibly

315 experienced a different climatic history due to its proximity to the monsoonal zone of southern Asia. It

316 is not thus surprising that it presents a different late glacial-Holocene hydrological evolution when

317 compared to the Eastern Mediterranean and Central Asia. Furthermore, as suggested by Roberts et al.

318 (2016), more than one lake record is required to disentangle the changes related to climate change from

319 those related to lake ontogeny. Before a general conclusion on lake hydrological changes in southern

320 Zagros can be drawn, other lake records should thus be established and compared and contrasted with

321 that of Arjan.

322 Southwest Asia shows a more complex hydroclimatic history compared to Europe, best

323 exemplified by the 'early Holocene precipitation paradox'. Indeed, the geochemical and pollen proxies

324 suggest different hydrological regimes dominated during the early Holocene. While geochemical data

325 suggest generally higher effective moisture, the pollen records indicate a limited expansion of deciduous

326 forest and thus generally drier conditions. A number of hypotheses have been evoked by different

327   scholars to explain this 'paradox' including a different precipitation seasonality in the early compared

328   to the late Holocene, a strong early human impact on forest and steppe forest ecosystems, or a mixture

329   of both (e.g. Stevens et al. 2001; Roberts 2002; Jones and Roberts 2008; Djamali et al. 2010). Part of

330   such conflicting interpretations stems from the fact that the current interpretations are mainly based only

331   on pollen and isotopic proxies. The new palaeohydrological indicators (fossil chironomid assemblages)

332   presented in this study furnish additional data on lake-level changes and can help in explaining the

333   hydrological paradoxes outlined above. The sensitivity of proxy records to local versus regional climate

334   variabilities also needs to be investigated to supplement the high potential of chironomids, which may

335   reflect changes in climate and hydrology at the local scale. The capacity of chironomid-based lake level

336   reconstructions to detect high frequency events during the Holocene should therefore be evaluated in

337   future palaeolimnological investigations.

338

339   Conclusions

340   The palaeoecological analysis of subfossil chironomid head capsules revealed a major change

341   in the hydrology of Dasht-e Arjan Wetland at the transition of the Younger Dryas to the onset of the

342   Holocene. In the absence of geochemical proxies from the studied sediment core, the chironomid data

343   helped to reconcile the palaeohydrology of this low-latitude wetland situated in the southern Zagros

344   Mountains. In the Zagros and adjacent highlands, although annual precipitation decreased in a similar

345   manner as the rest of the Northern Hemisphere, the hydrological consequences of lower annual

346   temperatures appear to have maintained higher amounts of water in the wetlands. During the YD, the

347   possible contribution of melt-water from local glaciers to Arjan wetland hydrology shows the necessity

348   to probe the late Quaternary history of glaciers in the Zagros Mountains. At present, it is unclear if such

349   glaciers provided significant water resources during the late glacial period. More late glacial records are

350   still required to understand the spatial patterns of hydrological change in the late Pleistocene-Holocene

351   transition before a regional picture of the hydroclimatic mechanisms driving these changes can be

352   drawn. Although the possible impacts of high effective moisture (high lake levels and aquifers) in the

353   Iranian highlands on the early Neolithic communities was not discussed in the present paper, the data

354 provided in this study, and similar investigations in the Fertile Crescent, will help to better understand

355 the possible roles and explanatory mechanisms in the processes of Neolithisation. In particular,

356 providing a palaeoenvironmental/palaeoclimate context for the beginning of plant/animal domestication

357 and the establishment of the first Neolithic sedentary populations is extremely important.

358   The chironomid-based hydrological reconstruction from Lake Arjan is encouraging. In the

359 future, more quantified data are required for comparisons with regional palaeoclimatic records e.g. the

360 Sea Surface Temperatures of the Arabian Sea or the speleothem records from Southern Asia, Northern

361 Iran, Arabia, and Turkey.

362

363 Acknowledgments

372   Reference

373   Aubert, C., .Brisset, E., Djamali, M., Sharifi, A., Ponel, P., Gambin, B., Akbari- Azirani, T., Guibal, F., Lahijani,
374   H., Naderi-Beni, A., de Beaulieu, J.-L., Pourmand, A., Andrieu-Ponel, V., Thiéry, A., and Gandouin, E. 2017.
375   Late glacial and early Holocene hydroclimate variability in northwest Iran (Talesh Mountains) inferred from
376   chironomid and pollen analysis. Journal of Paleolimnology, **58**: 151–167.

377   Ammann, B., Birks, H.J., Brooks, S.J., Eicher, U., von Grafenstein, U., Hofmann, W., Lemdahl, G., Schwander,
378   J., Tobolski, K., and Wick, L. 2000. Quantification of biotic responses to rapid climatic changes around the
379   Younger Dryas - a synthesis. Palaeogeography, Palaeoclimatology, Palaeoecology, **159**: 313–347.

380   Barley, E.M., Walker, I.R., Kurek, J., Cwynar, L.C., Mathewes, R.W., Gajewski, K., and Finney, B.P. 2006. A
381   northwest North American training set: distribution of freshwater midges in relation to air temperature and
382   lake depth. Journal of Paleolimnology, **36**: 295–314.

383   Blaauw, M. 2010. Methods and code for 'classical' age-modelling of radiocarbon sequences. Quaternary
384   geochronology, **5**: 512–518.

385   Blockley, S.P.E., and Pinhasi, R. 2011. A revised chronology for the adoption of agriculture in the Southern Levant
386   and the role of Lateglacial climatic change. Quaternary Science Reviews, **30**: 98–108.

387   Brodin, Y.W. 1986. The postglacial history of Lake Flarken, southern Sweden, interpreted from subfossil insect
388   remains. Internationale Revue der Gesamten Hydrobiologie, **71**: 371–432.

389   Brooks, S.J., Langdon, P.G., and Heiri, O. 2007. The identification and Use of Palaeartic Chironomidae Larvae in
390   Palaeoecology. Technical Guide Nº10. Quaternary Research Association, London.

391   Broushaki, F., Thomas, M.G., Link, V., López, S., van Dorp, L., Kirsanow, K., Hofmanová, Z., Diekmann, Y.,
392   Cassidy, L.M., and Díez-del-Molino, D. 2016. Early Neolithic genomes from the eastern Fertile Crescent.
393   Science, **353**: 499–503.

394   Chang, J., Zhang, E., Liu, E., and Shulmeister, J. 2017. Summer temperature variability inferred from subfossil
395   chironomid assemblages from the south-east margin of the Qinghai–Tibetan Plateau for the last 5000 years.
396   The Holocene, **27**: 1876–1884.

397   Djamali, M., Akhani, H., Andrieu-Ponel, V., Braconnot, P., Brewer, S., Beaulieu, J.-L., Fleitmann, D., Fleury, J.,
398   Gasse, F., Guibal, F., Jackson, S.T., Lézin,e A.-M., Médail, F., Ponel, P., Roberts, N., and Stevens, L. 2010.

399   Indian Summer Monsoon variations could have affected the early-Holocene woodland expansion in the Near

400   East. The Holocene, **20**: 813–820.

401   Djamali, M., Akhani, H., Khoshravesh, R., Andrieu-Ponel, V., Ponel, P., and Brewer, S. 2011. Application of the

402   global bioclimatic classification to Iran: implications for understanding the modern vegetation and

403   biogeography. Ecologia Mediterranea, **37**: 91–114.

404   Djamali, M., Baumel, A., Brewer, S., Jackson, S.T., Kadereit, J.W., López-Vinyallonga, S., Mehregan, I.,

405   Shabanian, E., and Simakova, A. 2012. Ecological implications of Cousinia Cass. (Asteraceae) persistence

406   through the last two glacial–interglacial cycles in the continental Middle East for the Irano-Turanian flora.

407   Review of Palaeobotany and Palynology, **172**: 10–20.

408   Djamali, M., Gondet, S., Ashjari, J., Marriner, N., Aubert, C., Brisset, E., Longerey, J., Mashkour, M., Miller,

409   N.F., Naderi-Beni, A., Pourkerman, M., Rashidian, E., Rigot, J.-B., Shidrang, S., Thiéry, A., and Gandouin,

410   E. 2018. Karstic-spring wetlands of the Persepolis Basin, SW Iran: unique sediment archives of Holocene

411   environmental change and human impacts. Canadian Journal of Earth Science. doi/10.1139/cjes-2018-0065.

412   Ebrahimi, B., and Seif, A. 2016. Equilibrium-Line Altitudes of Late Quaternary Glaciers in the Zardkuh Mountain.

413   Geopersia, **6(2)**: 299-322.

414   Eggermont, H., Heiri, O., and Verschuren, D. 2006. Fossil Chironomidae (Insecta: Diptera) as quantitative

415   indicators of past salinity in African lakes. Quaternary Science Reviews, **25**: 1966–1994.

416   Eggermont, H., De Deyne, P., and Verschuren, D. 2007. Spatial variability of chironomid death assemblages in

417   the surface sediments of a fluctuating tropical lake (Lake Naivasha, Kenya). Journal of Paleolimnology, **38**:

418   309–328.

419   Engels, S., and Cwynar, L.C. 2011. Changes in fossil chironomid remains along a depth gradient: evidence for

420   common faunal thresholds within lakes. Hydrobiologia 665, 15–38.

421   Fleitmann, D., Burns, S.J., Mangini, A., Mudelsee, M., Kramers, J., Villa, I., Neff, U., Al-Subarry, A., Buettner,

422   A., Hippler, D., and Matter, A. 2007. Holocene ITCZ and Indian monsoon dynamics recorded in stalagmites

423   from Oman and Yemen (Socotra). Quaternary Science Reviews, **26**: 170–188.

424   Gandouin, E., Franquet, E., and Van Vliet-Lanoe, B. 2005. Chironomids (Diptera) in River Floodplains: their

425   Status and Potential Use for Palaeoenvironmental Reconstruction Purposes. Archiv für Hydrobiologie, **162**:

426   511–534.

427   Grimm, E.C. (1987) CONISS: A FORTRAN 77 program for stratigraphically constrained cluster analysis by the

428   method of incremental sum of squares. Computers & Geosciences, **13**: 13–35.

429   Heiri, O., Brooks, S.J., Birks, H.J.B., and Lotter, A.F. 2011. A 274-lake calibration dataset and inference model

430   for chironomid-based summer temperature reconstruction in Europe. Quaternary Science Reviews, **30**: 3445–

431   3456.

432   Heiri, O., and Lotter, A.F. 2001. Effect of low count sums on quantitative environmental reconstructions: an

433   example using subfossil chironomids. Journal of Paleolimnology, **26**: 343–350.

434   Henrikson, L., Olofsson, J.B., and Oscarson, H.G. 1982. The impact of acidification on Chironomidae (Diptera)

435   as indicated by subfossil stratification. Hydrobiologia, **86**: 223-229.

436   Hoek, W.Z., Yu, Z.C., and Lowe, J.J. 2008. INTegration of Ice-core, MArine, and TErrestrial records

437   (INTIMATE): refining the record of the Last Glacial–Interglacial Transition. Quaternary Science Reviews,

438   **27**: 1–5.

439   Hosseini, Z., Khaledi, S., and Naderi-Beni, A. 2017. Reconstruction of vegetation and palaeoclimate of Dasht-e

440   Arjan, Fars, during the late Pleistocene and Holocene based on pollen analysis. Journal of climatological

441   studies, **27-28**: 87–98 (paper in Persian language).

442   Jones, M. D., and Roberts, C. N. 2008. Interpreting lake isotope records of Holocene environmental change in the

443   Eastern Mediterranean. Quaternary International, **181**: 32–38.

444   Juggins, S. 2007. C2 Version 1.5 User guide. Software for ecological and palaeoecological data analysis and

445   visualisation. NewcastleUniversity, Newcastle upon Tyne, UK. 73pp.

446   Juggins, S. (2017) rioja: Analysis of Quaternary Science Data, R package version (0.9-15.1). (http://cran.r-

447   project.org/package=rioja).

448   Langdon, P., Ruiz, Z., Wynne, S., Sayer, C., and Davidson, T. 2010. Ecological influences on larval chironomid

449   communities in shallow lakes: implications for palaeolimnological interpretations. Freshwater Biology, **55**:

450   531–545.

451 Lowe, J.J., and Walker, M.J.C. 1997. Reconstructing Quaternary Environments, 2 edition. ed. Routledge, Harlow.

452 Luoto, T.P., Ojala, A.E.K., Arppe, L., Brooks, S.J., Kurki, E., Oksman, M., Wooller, M.J., and Zajączkowski, M.
453   2018. Synchronized proxy-based temperature reconstructions reveal mid- to late Holocene climate
454   oscillations in High Arctic Svalbard. Journal of Quaternary Science, **33**: 93–99.

455 Matthews, R., and Fazeli Nashli, H. 2013. The neolithisation of Iran. Oxbow Books. Oxford (Royaume Uni).

456 Mayewski, P.A., Meeker, L.D., Twickler, M.S., Whitlow, S., Yang, Q., Lyons, W.B., and Prentice, M. 1997. Major
457   features and forcing of high254 P.A. Mayewski et al. / Quaternary Research 62 (2004) 243–255 latitude
458   northern hemisphere atmospheric circulation using a 110,000- year long glaciochemical series. Journal of
459   Geophysical Research, **102**: 26345–26366.

460 Milanovic, P., and Aghili, B. 1990. Hydrogeological characteristics and groundwater mismanagement of kazerun
461   karstic aquifer, Zagros, Iran. Hydrogeological Processes in Karst Terranes, **10**: 163–171.

462 North Greenland Ice Core Project members. 2004. High-resolution record of Northern Hemisphere climate
463   extending into the last interglacial period. Nature, **431(7005)**: 147–151.

464 Pinder, L.C.V., and Reiss, F. 1983. The Larvae of Chironominae (Diptera: Chironomidae) of the Holartic region.
465   Keys and diagnoses. Entomol Scand Supplement, **19**: 293–435.

466 R Core Team 2012. R: A language and environment for statistical computing. R Foundation for Statistical
467   Computing, Vienna, Austria.

468 Rasmussen, S.O., Andersen, K.K., Svensson, A.M., Steffensen, J.P., Vinther, B.M., Clausen, H.B., Siggaard-
469   Andersen, M.-L., Johnsen, S.J., Larsen, L.B., Dahl-Jensen, D., Bigler, M., Rothlisberger, R., Fischer, H.,
470   Goto-Azuma, K., Hansson, M.E., and Ruth, U. 2006. A new Greenland ice core chronology for the last glacial
471   termination. Journal of Geophysical Research, **111**. doi:10.1029/2005JD006079.

472 Reimer, P.J., Bard, E., Bayliss, A., Beck, J.W., Blackwell, P.G., Ramsey, C.B., Buck, C.E., Cheng, H., Edwards,
473   R.L., Friedrich, M., Grootes, P.M., Guilderson, T.P., Haflidason, H., Hajdas, I., Hatté, C., Heaton, T.J.,
474   Hoffmann, D.L., Hogg, A.G., Hughen, K.A., Kaiser, K.F., Kromer, B., Manning, S.W., Niu, M., Reimer,
475   R.W., Richards, D.A., Scott, E.M., Southon, J.R., Staff, R.A., Turney, C.S.M., and van der Plicht, J. 2013.
476   IntCal13 and Marine13 Radiocarbon Age Calibration Curves 0–50,000 years cal BP. Radiocarbon, **55**: 1869–
477   1887.

478 Riehl, S., Zeidi, M., and Conard, N.J. 2013. Emergence of Agriculture in the Foothills of the Zagros Mountains of
479   Iran. Science, **341**: 65–67.

480 Roberts, N. 2002. Did prehistoric landscape management retard the post-glacial spread of woodland in Southwest
481   Asia? Antiquity, **76**: 1002–1010.

482 Roberts, N., Allcock, S.L., Arnaud, F., Dean, J.R., Eastwood, W.J., Jones, M.D., Leng, M.J., Metcalfe, S.E., Malet,
483   E., Woodbridge, J., and Yiğitbaşıoğlu, H. 2016. A tale of two lakes: a multi-proxy comparison of Lateglacial
484   and Holocene environmental change in Cappadocia, Turkey: A TALE OF TWO LAKES. Journal of
485   Quaternary Science, **31**: 348–362.

486 Seyrafian, A., Vaziri-Moghaddam, H., Arzani, N., and Taheri, A. 2011. Facies analysis of the Asmari Formation
487   in central and north-central Zagros basin, southwest Iran: Biostratigraphy, paleoecology and diagenesis.
488   Revista Mexicana de Ciencias Geológicas, **28(3)**: 439–458.

489 Sharifi, A., Pourmand, A., Canuel, E.A., Ferer-Tyler, E., Peterson, L.C., Aichner, B., Feakins, S.J., Daryaee, T.,
490   Djamali, M., Beni, A.N., Lahijani, H.A.K., and Swart, P.K. 2015. Abrupt climate variability since the last
491   deglaciation based on a high-resolution, multi-proxy peat record from NW Iran: The hand that rocked the
492   Cradle of Civilization? Quaternary Science Reviews, **123**: 215–230.

493 Sharifi, A., Murphy, L.N., Pourmand, A., Clement, A.C., Canuel, E.A., Naderi Beni, A., A.K. Lahijani, H.,
494   Delanghe, D., and Ahmady-Birgani, H. 2018. Early-Holocene greening of the Afro-Asian dust belt changed
495   sources of mineral dust in West Asia. Earth and Planetary Science Letters, **481**: 30–40.

496 Stevens, L.R., Wright, H.E. Jr., and Ito, E. 2001. Proposed changes in seasonality of climate during the Lateglacial
497   and Holocene at Lake Zeribar, Iran. The Holocene, **11**: 747–755.

498 Stevens, L.R., Ito, E., Schwalb, A., and Wright, H.E. Jr. 2006. Timing of atmospheric precipitation in the Zagros
499   Mountains inferred from a multi-proxy record from Lake Mirabad, Iran. Quaternary Research, **66**: 494–500.

500 Verneaux, V., and Aleya, L. 1998. Bathymetric distributions of chironomid communities in ten French lakes:
501   Implications on lake classification. Fundamental and Applied Limnology, **142**: 209–228.

502 Wang, H., Chen, J., Zhang, S., Zhang, D.D., Wang, Z., Xu, Q., Chen, S., Wang, S., Kang, S., and Chen, F. 2018.
503   A chironomid-based record of temperature variability during the past 4000 years in northern China and its
504   possible societal implications. Climate of the Past, **14**: 383–396.

505   Willcox, G. 2012. The beginnings of cereal cultivation and domestication in Southwest Asia. In D. Potts (ed.) A

506   companion to the archaeology of the ancient Near East. Wiley Blackwell Malden, Oxford.

507   Zhang, E., Jones, R., Bedford, A., Langdon, P., and Tang, H. 2007. A chironomid-based salinity inference model

508   from lakes on the Tibetan Plateau. Journal of Paleolimnology, **38**: 477–491.

509   **Table:**

510

511   Table 1. [14]C ages obtained and the type of corresponding material (Lake Arjan). Calibrated ages are reported with
512   2-σ ranges. Excluded ages are marked in *italics*.

Laboratory code	Depth (cm)	Material	Age years BP (^{14}C)	Age years cal BP (2σ interval)
Poz-Arj148	148	Organic mud	6430 ± 50	7356 (7274-7429)
Poz-Arj478	*478*	*Calcareous mud (bulk)*	*9280 ± 50*	*10455 (10287-10612)*
Poz-Arj503	503	Gyttja (bulk)	7940 ± 50	10715 (10573-10844)
Poz-Arj614	614	Gyttja (bulk)	10180 ± 50	11869 (11631-12060)
Poz-Arj671	671	Gyttja (bulk)	11880± 60	12408 (12255-12536)
Poz-*Arj756*	*756*	Plant remains	*11370± 60*	*13212 (13099-13332)*

513

514 **Figure captions:**

515

516 Figure 1: A. Location of Dasht-e Arjan Wetland and Lake Neor in Iranian plateau. B. The fault system
517 controlling the subsidence of the Arjan Basin with the position of the coring site. C. Climate diagram of
518 Shiraz. D. Dasht-e Arjan during a lowstand with the position of coring site (Source: Google Earth;
519 Landsat/Copernicus (B dating to 12/1987) and CNES/Airbus (C dating to 12/2016)).

520

521 Figure 2. Lithostratigraphic log and age-depth model for the whole core (upper right) with a detailed
522 focus on the studied section from Dasht-e Arjan Wetland. The chironomid record presented here
523 corresponds to the depths of 630 to 550 cm (12 000 to 11 200 years cal BP).

524

525 Figure 3. Synthetic subfossil chironomid diagram from the Lake Arjan record (left) compared to pollen
526 records for the same section of the same core (see Hosseini et al., 2017 for a detailed pollen diagram).
527 The zonation pollen diagram was made visually. Profundal taxa: inhabit profundal zones of lake. Littoral
528 taxa: inhabit littorals margins of lake. Other taxa: indifferent to depth or no documented ecological
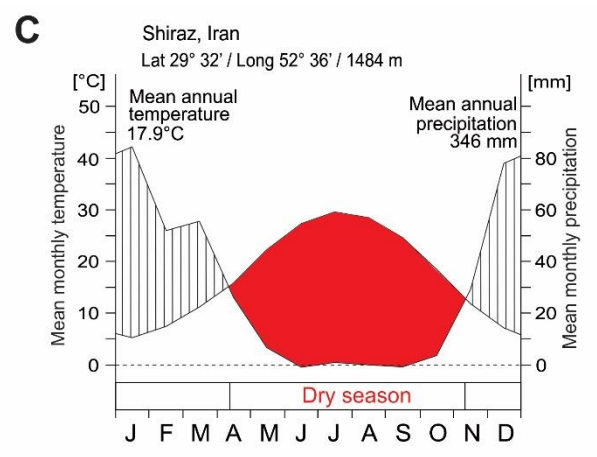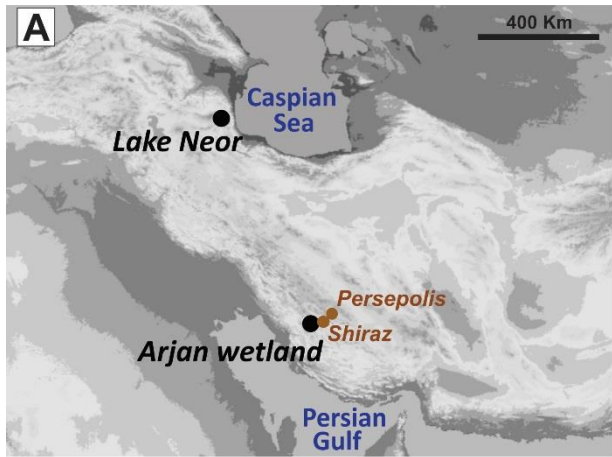529 affinities.

530

531 Figure 4. Scatter plots for PCA scores of chironomid assemblages in the late glacial-Early Holocene
532 transition sediments of Dasht-e Arjan Wetland core showing the variable factor map of PCA (A) and
533 contribution of different variables (taxa) to axis 1 (B) and axis 2 (C).
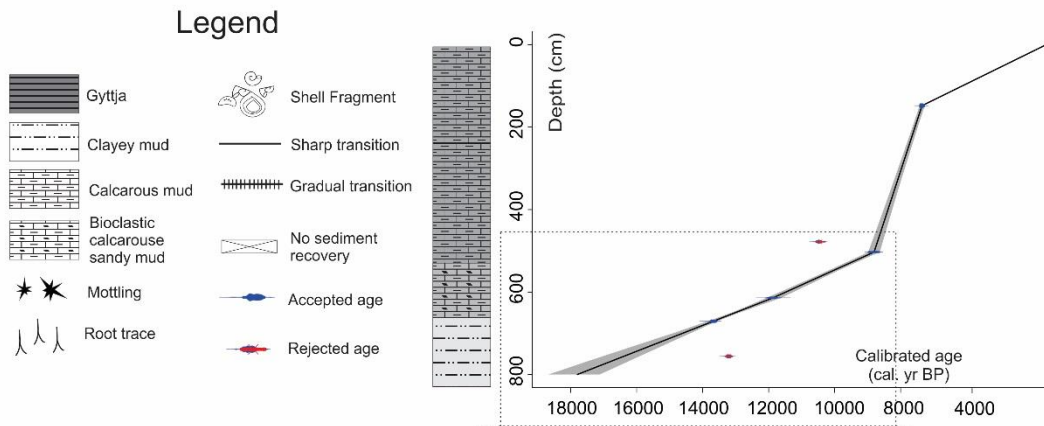
534

535 Figure 5. Comparison of the abundance of the sum of the deep water chironomid taxa between Lake
536 Arjan and Lake Neor (Aubert et al. 2017) compared with temperature variations in Greenland (NGRIP
537 record: North Greenland Ice Core Project members (2004) and aeolian activity in Lake Neor (Sharifi et
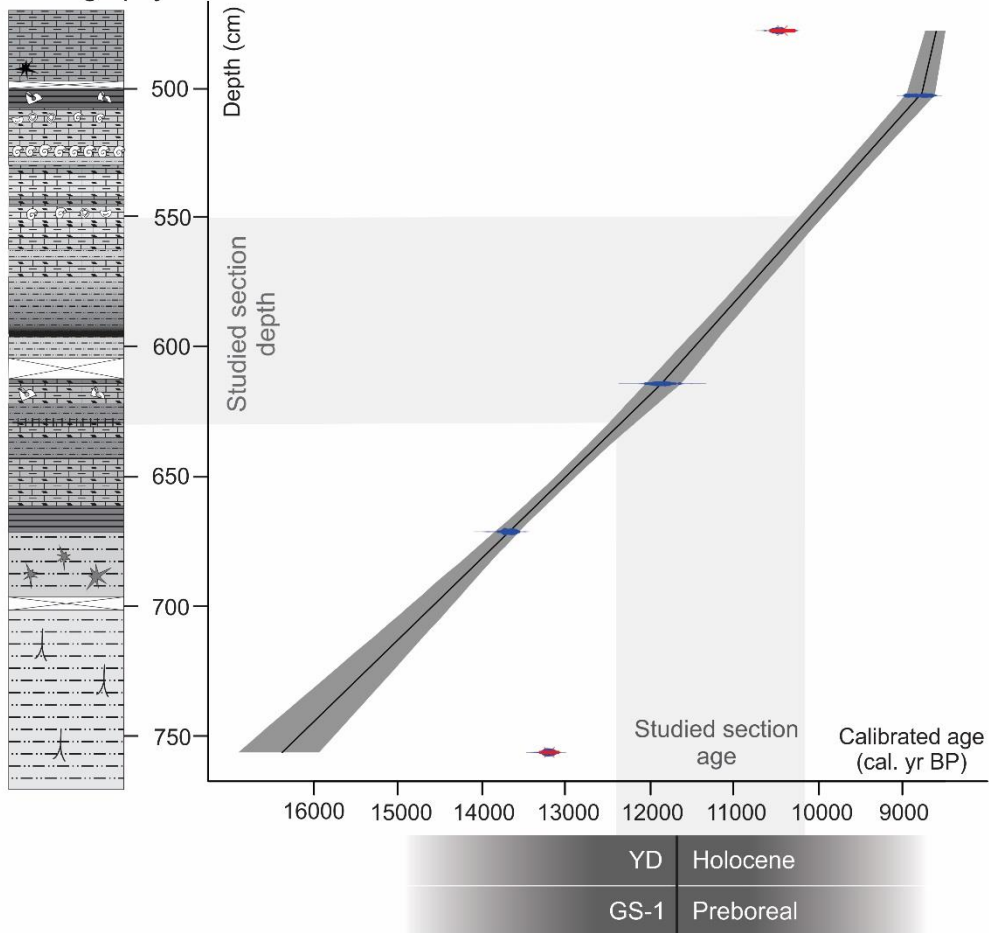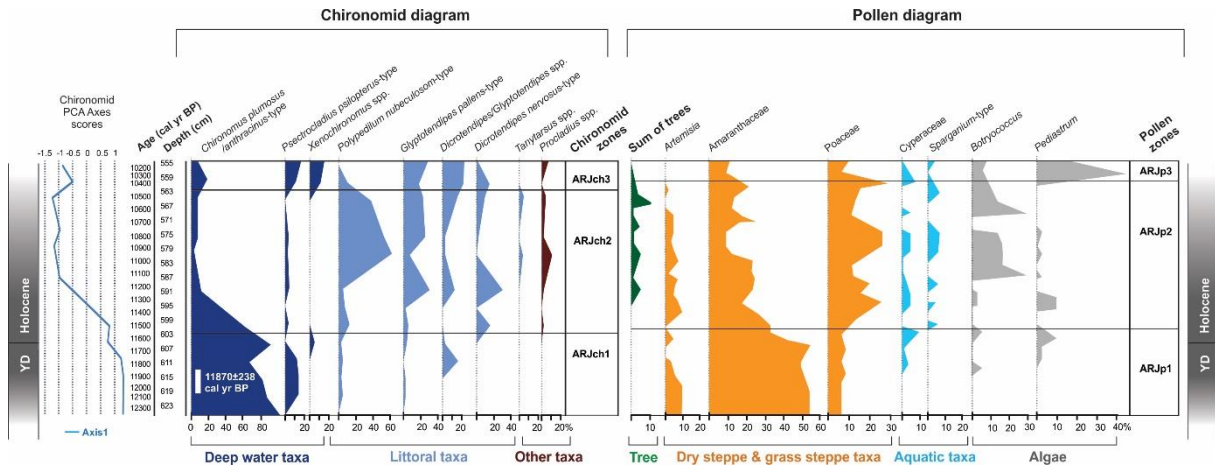538 al. 2015).

539

540

541

542

543

544
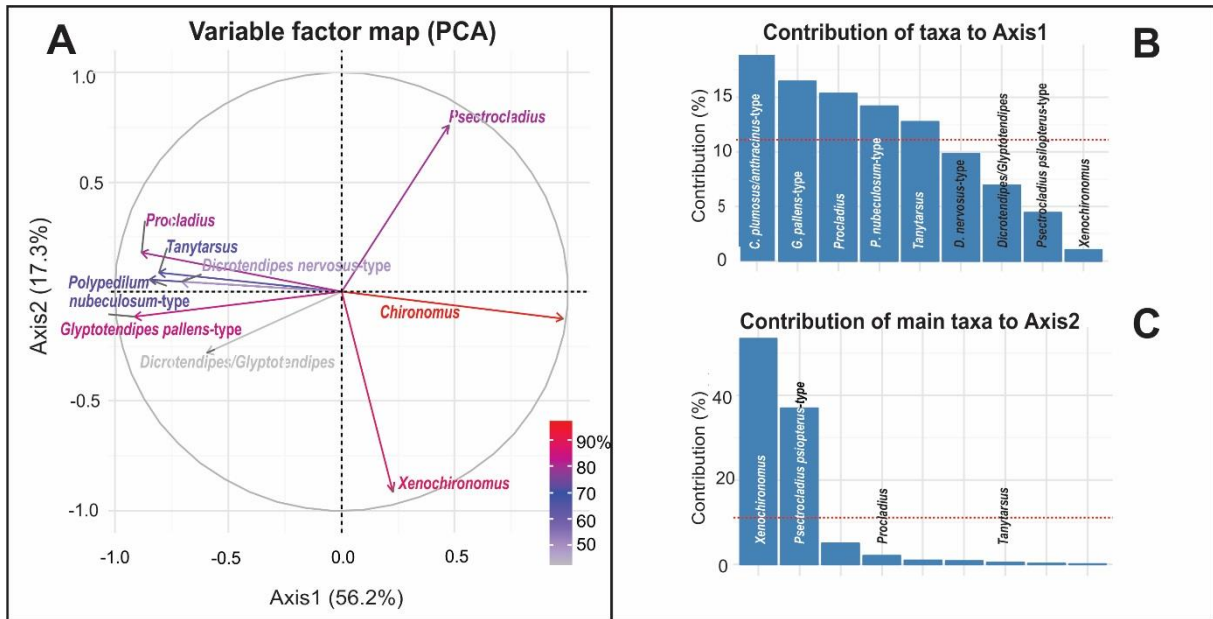
545

546

547

548